COMPUTATION OF TRAVEL TIMES AND STATION CORRECTION SURFACES IN EURASIA USING THREE DIMENSIONAL VELOCITY MODELS

A. Villaseñor, M.H. Ritzwoller, M.P. Barmin, E.R. Engdahl, and A.L. Levshin

Department of Physics, University of Colorado, Campus Box 390, Boulder, CO 80309

ABSTRACT

We have investigated the performance of a variety of travel time computation methods for application in highly heterogeneous three-dimensional (3-D) velocity structures, such as those found in Central Eurasia. Recent 3-D models of the crust and upper mantle beneath Central Eurasia (e.g., Villaseñor et al., 2000) contain sharp vertical and horizontal velocity contrasts and thin layers which complicate the accurate computation of travel times.

Techniques based on ray-perturbation theory or the graph method (e.g., Pulliam and Snieder, 1996; Nolet and Moser, 1993) do not appear to work well when the velocity anomalies are large relative to the reference model. In these cases the reference ray can be very different from the minimum-time ray, and the methods fail to converge rapidly and in some cases do not converge at all to the global minimum.

Ray shooting and finite-difference algorithms are more computationally expensive, but provide accurate results in the presence of large velocity contrasts. In the ray-shooting method, the model is parameterized in terms of smooth polynomials in all directions. Ray-shooting methods are normally implemented only in 2-D (e.g., Červený and Pšenčík, 1988), and do not consider propagation paths off the sagittal plane. The finite difference method computes travel times for first-arriving phases for the entire model (e.g., Podvin and Lecomte, 1991). Rays are obtained afterward by back-tracing from any point inside the model (receiver) to the source. This method is 3-D and the model is parameterized in terms of constant-velocity cubic cells. The accuracy of the travel times is determined by the cell size. Computer memory effectively limits the minimum cell size for a given region but this constraint can be overcome by computing travel times in 2-D.

Ray shooting and finite difference methods produce similar travel times, but differences can locally be greater than 1 s largely due to the differences in model parameterization between the two methods. We report estimates of uncertainties in travel times and station correction surfaces between these two methods and also discuss the effect of computing travel times in 2-D rather than in 3-D.

For IMS stations in Central Eurasia we present travel time correction surfaces relative to the 1-D model ak135 predicted by the 3-D velocity model of Villaseñor et al. (2000). At epicentral distances less than about 10 degrees, the character of the correction surfaces is dominated by the difference in crustal thickness between the 3-D model and ak135. Beyond 5-10 degrees, velocity variations in the uppermost mantle become increasingly important.

Key Words: Travel times, ray tracing, source-specific station corrections, SSSC.

OBJECTIVE

The objective of this research is to evaluate methods for computing travel times at regional distances for three dimensional velocity models, and assess their usefulness to produce model-predicted source-specific station corrections (SSSCs) for IMS stations in Central Eurasia.

RESEARCH ACCOMPLISHED

Introduction

Locating low magnitude events with the accuracy required by CTBT monitoring is a challenging task. These events are normally recorded only at regional distances, where the effect of crustal and upper mantle structure on seismic travel times is important. One-dimensional (1-D), radially-symmetric models such as iasp91 (Kennett and Engdahl, 1991) or ak135 (Kennett et al., 1995) cannot predict travel times accurately for local and regional distances. A method to account for the effects of lateral heterogeneity at a given station is to construct source-specific station corrections or SSSCs. Empirical SSSCs can be constructed in regions where calibration data such as explosions and/or well located earthquakes are available (e.g., Bondár et al., 1999). Unfortunately this is normally not the case, and large regions of the Earth have little or no calibration data. For these regions, SSSCs can be obtained using available regional and/or global velocity models. To obtain these model-predicted SSSCs, rays have to be traced through the model, from each station to points on a specified rectangular latitude/longitude grid, within a given distance from the station (normally 20 degrees). Therefore, accurate and efficient methods to calculate travel times in 3-D velocity models are required.

Computation of travel times in heterogeneous media is a complicated problem. This complexity is illustrated by the large number of methodologies developed, and by the fact that each one has its advantages and shortcomings (for a review see for example Červený, 1987). We have restricted this study to three families of methods: ray bending, ray shooting, and finite difference methods. Bending methods are generally fast and work well for smoothly varying velocity models, but may converge toward local travel time minima. Shooting methods work better for more heterogeneous models, but at the expense of computation time, and they cannot trace rays in shadow zones. Finite difference methods can provide very accurate results even in presence of extreme velocity variations, but require small cell sizes. Finite difference methods normally produce travel times for first arriving phases, and not for later phases.

The two bending codes tested in this study are described by Bijwaard and Spakman (1999). The first code is an implementation of the graph method by Nolet and Moser (1993) based on the work of Moser (1991). The second code is based on ray perturbation theory, and was developed by Pulliam and Snieder (1996) based on the original implementation of Snieder and Sambridge (1993). Both codes perform 3-D ray tracing and work well for models with small velocity perturbations (e.g. Bijwaard et al., 1998). However, they do not work with other models (e.g., Villaseñor et al., 2000) that contain sharp vertical discontinuities, thin layers, and large lateral velocity variations. These two codes have not been used in the results presented in this study.

We have also tested the ray shooting code of Červený and Pšenčík (1988). This is a 2-D method, for laterally-varying layered models. The geometry of the layers is described in terms of splines. Computations are made in a cartesian (flat Earth) reference system, and applying an earth-flattening transformation.

Finally we have tested the finite difference technique of Podvin and Lecomte (1991). This method can be used both in 3-D and 2-D. The model is parameterized in terms of cubic constant-velocity cells. Therefore, models described using a spherical parameterization have to be mapped into a cartesian reference system, resulting in some inefficiency in the amount of memory required to store the model. Travel time wavefronts and not rays are computed in this method. Rays can be obtained a posteriori by backtracking towards the source following the normal direction to the wavefronts.

Accuracy tests

We have conducted tests to evaluate the performance and accuracy of the ray shooting and finite difference methods. First we test these methods against theoretical travel times for the one-dimensional, radially-symmetric model ak135 (Kennett et al., 1995). Second we compare the results of both methods in 2-D, using vertical cross-sections of the S model of Villaseñor et al. (2000), and finally we compare the performance of 2-D versus full 3-D travel times.

To evaluate the accuracy of the ray shooting and finite difference methods, we compare their results with theoretical travel times (Buland and Chapman, 1983) for ak135. The results of these comparisons are shown in Figure 1. In

this case the ray shooting method is very precise, better that 0.1 s. The accuracy of the finite difference method depends on the cell size. For a cell size of 1 x 1 km the precision is also better than 0.1 s. If the cell size is increased to 2 x 2 km the precision is still better that 0.25 second, but some artifacts caused by the finite difference model parameterization (2 x 2 km constant velocity cells) can be seen. When the first arrival changes from Pg to Pn (at approximately 1.5 degrees) there is a baseline shift of 0.1 s (Figure 1). This shift is caused because Moho depth in the finite difference model parameterization of 2 x 2 km cells is 36 km, instead of 35 km in ak135.

We have compared the 2-D ray shooting method and the finite difference method using two great-circle vertical cross sections through the S model of Villaseñor et al. (2000) for Central Eurasia. This model is transversely isotropic in the uppermost mantle, but for this test we have used the v_{SV} component of the model, which is better constrained than v_{SH}. The differences between travel times using both methods for the two great circle paths considered are shown in Figure 2. The differences are on the order of 2 seconds, much larger than the tests performed with the 1-D model ak135. We find that these differences are caused by the way the 3-D model is translated into the internal parameterization of each travel time code. In some other cases, not shown here, the differences are much larger, and caused by the failure of the ray-shooting method to find the minimum travel time ray path. In most cases, modifying the parameters that control the accuracy of the ray shooting solution eliminates these problems, but at the expense of longer computation time. On the other hand, the finite difference method is very fast and efficient, and always provides the first arrival time even in presence of extreme velocity contrasts (Podvin and Lecomte, 1991).

Finally we have investigated the importance of full 3-D travel time computation versus computations in 2-D. For this test we only use the finite-difference method of Podvin and Lecomte (1991) because the ray shooting code is strictly 2-D. To evaluate the differences between 3-D and 2-D travel times we have considered two profiles through the S model of Villaseñor et al. (2000). Figure 3 shows the differences between the computed 3-D and 2-D travel times. These differences are small (less than 2 seconds), and similar in magnitude to the differences between both 2-D codes shown in Figure 2. Full 3-D ray-tracing is important for non-linear tomography studies, allowing to obtain improved, more focused velocity models (Bijwaard and Spakman, 2000; Widiyantoro et al., 2000), but for the model considered here and for regional distances it is not necessary for computing travel times and SSSCs with sufficient precision. This is probably because the model we have used is more heterogeneous vertically (with thin layers and sharp velocity contrasts) than laterally, and therefore off-great circle propagation is not very important.

Effects of the reference model on the computation of SSSCs

Global velocity models obtained by inversion of large datasets of arrival times of seismic phases (e.g., Bijwaard et al., 1988), are normally described as perturbations to 1-D models such as iasp91 or ak135. These 3-D models provide high resolution in regions with high density of earthquakes and stations but contain large gaps in regions where seismicity is low and/or stations do not exist. On the other hand, models that use surface wave and normal mode data have lower resolution than models based on body waves, but their coverage is more homogeneous. These models are normally described as perturbations relative to PREM (Dziewonski and Anderson, 1981)

There are some significant differences between PREM and ak135 in the crust and upper mantle. PREM is designed as an average Earth model, and contains a 3 km thick water layer, with Moho located at 24.4 km depth. The crust in ak135 is of continental type (because most of seismic stations are located on continents), with a Moho depth of 35 km. In the uppermost mantle, between Moho and 220 km, PREM is transversely isotropic, and exhibits a well-developed low velocity zone, while ak135 is isotropic and lacks a low velocity zone, although the velocity gradient in the uppermost mantle is very small for both P and S. In the upper mantle PREM has a velocity discontinuity at 220 km depth which is much sharper for P than for S. This discontinuity is absent in ak135. Finally the transition zone is 20 km thicker for PREM (400 – 670 km) than for ak135 (410 – 660 km).

These differences between PREM and ak135 obviously translate into different travel times at regional distances, as shown in Figure 4. We have calculated the difference in travel times between PREM and ak135 for a source located at 40 km depth, and for receivers also at 40 km depth. This has been done to avoid additional complications by differences in crustal structure. Therefore, the curves shown in Figure 4 represent the effect of differences in upper mantle and transition zone structure between the two models. Immediately below Moho v_{PH} for PREM is larger than v_P for ak135. As a result PREM travel times for v_{PH} are faster (smaller) than ak135, and this can be observed as

increasingly negative values in Figure 4 (top panel, solid line). The difference in travel time reaches a minimum of approximately –3 s at distances of 14 degrees, and then decreases to 0 at 25 degrees. The situation is reversed for PREM v_{PV}. Immediately below Moho v_{PV} for PREM is slightly smaller v_P for ak135 and this results in positive values, indicating that travel times for PREM v_{PV} are slower (larger) than ak135 (top panel, dashed line). The same pattern can be observed for S wave travel times (Figure 4, bottom). In this case the differences in travel times are larger (-8 s for PREM v_{SH}) and the maximum values of the differences occur at different distances (e.g., at 19 degrees for PREM v_{SH}).

SSSCs are normally referred to iasp91 or ak135 (for the purpose of regional travel times both models are identical) but many global and regional models are expressed as perturbations relative to PREM. Because of the differences in travel times between PREM and ak135 we must expect artifacts in the SSSCs that are caused by the choice of the reference model, in addition to features due to lateral heterogeneity. Figure 5a shows the SSSC relative to ak135 for auxiliary IMS station AAK (Ala-Archa, Kyrgyzstan) computed from the S model of Villaseñor et al. (2000). At epicentral distances less than about 10 degrees, the character of the correction surface is dominated by the difference in crustal thickness between the 3-D model and ak135. The crust in Central Eurasia is thicker than 35 km, and this results in positive station corrections (slower travel times than ak135). Beyond 5-10 degrees, velocity variations in the uppermost mantle become increasingly important. High velocities in the Indian craton produce large negative corrections (faster travel times than ak135). This effect can also be observed in the East European platform, north of the Caspian Sea. On top of these features caused by lateral heterogeneity there is a ring of negative values, centered on the station and with a radius of approximately 20 degrees. As shown in Figure 4, this ring can be explained by the differences between our upper mantle model (which uses PREM as reference model) and ak135.

To avoid these artifacts, the SSSCs can be calculated relative to the model beneath the station, instead of relative to iasp91 or ak135. This guarantees that the velocity discontinuities of the 3-D model and reference model are located exactly at the same depths. Figure 5b shows the results of applying this procedure to AAK. The ring with negative values has disappeared, the shape of the correction surface is smoother and better correlated with the features of the 3-D model. Figure 5c shows the difference between the two correction surfaces obtained for AAK (Figures 5a and 5b). This clearly illustrates that the ring is an artifact caused by the choice of the reference model.

CONCLUSIONS AND RECOMMENDATIONS

We have tested the performance of travel time codes based on ray bending, ray shooting and finite differences for computing model-predicted SSSCs. For three-dimensional Earth models with large lateral and vertical velocity variations ray shooting and finite differences provide the best results.

For laterally heterogeneous models, the differences in computed travel times between different codes can be rather large (up to 2 seconds for regional distances). In some cases this can be caused by poor performance of one the methods (for example not being able to find the minimum travel time path, and converging to a local minimum). However, in the examples presented here, the differences are caused by differences in the internal model parameterization of each travel time code. These differences can be even larger if the influence of model uncertainties on the computation of travel times is considered.

Full 3-D ray tracing is important for non-linear tomography studies, allowing to obtain improved, more focused velocity models. However, 3-D travel times are not necessary for computing regional SSSCs. Tests indicate that, for models like the ones used in this study, travel time differences between 2-D and 3-D ray tracing are similar in magnitude to differences between travel time codes. In the future, when higher-resolution, more heterogeneous models become available, 3-D ray tracing may be required.

The choice of the reference model is extremely important for determining the features of model-predicted SSSCs. To ensure smoothly varying SSSCs, the 3-D model should have the upper mantle and transition zone discontinuities at the same depth as the reference model. Otherwise, the computed SSSCs may display large artifacts, that manifest as circular features (positive or negative in sign) centered on the station. These artifacts can be eliminated by using the model beneath the station as the reference model for the computation of the SSSCs.

Finally, methods need to be developed to evaluate the uncertainties of travel times and SSSCs based upon the uncertainties in the travel time methods and in the 3-D velocity models.

REFERENCES

Bijwaard, H., and W. Spakman, Fast kinematic ray tracing of first- and later-arriving global seismic phases, Geophys. J. Int., 139, 359-369, 1999.

Bijwaard, H., and W. Spakman, Non-linear global P-wave tomography by iterated linearized inversion, Geophys. J. Int., 141, 71-82, 2000.

Bijwaard, H., Spakman, W., and Engdahl, E.R., Closing the gap between regional and global travel time tomography, J. Geophys. Res., 103, 30055-30078, 1998.

Bondár, I., X. Yang, K. McLaughlin, R.G. North, V. Ryaboy, and W. Nagy, Source specific station corrections for regional phases at IMS stations in North America and Fennoscandia, Eos Trans. AGU, 79, 555, 1999.

Buland, R., and C.H. Chapman, The computation of seismic travel times, Bull. Seism. Soc. Am., 73, 1271-1302, 1983.

Červený, V., Ray tracing algorithms in three-dimensional laterally varying layered structures, in: Seismic Tomography, edited by G. Nolet, pp. 99-133, Reidel, Dordrecht, The Netherlands, 1987.

Červený, V., and I. Pšenčík,, Numerical modeling of seismic wave fields in 2-D laterally varying layered structures by the ray method, in Seismological Algorithms, Academic Press, London, 1988.

Dziewonski, A.M., and D.L. Anderson, Preliminary reference Earth model, Phys. Earth Planet. Inter., 25, 297-356, 1981.

Engdahl, E.R., R. van der Hilst, and R. Buland, Global teleseismic earthquake relocation with improved travel times and procedures for depth determination, Bull. Seism. Soc. Am., 88, 722-743, 1998.

Engdahl, E.R., and M.H. Ritzwoller, Crust and upper mantle P- and S-wave delay times at Eurasian seismic stations, Phys. Earth Planet. Int., submitted, 2000.

Kennett, B.L.N., and E.R. Engdahl, Travel times for global earthquake location and phase identification, Geophys. J. Int., 105, 429-465, 1991.

Kennett, B.L.N., E.R. Engdahl, and R. Buland, Constraints on seismic velocities in the Earth from travel times, Geophys. J. Int., 122, 108-124, 1995.

Moser, T.J., Shortest path calculation of seismic rays, Geophysics, 56, 59-67, 1991.

Nolet, G., and T.J. Moser, Teleseismic delay times in a 3-D Earth and a new look at the S discrepancy, Geophys. J. Int., 114, 185-195, 1993.

Podvin, P., and Lecomte, I., Finite difference computation of travel times in very contrasted velocity models: a massively parallel approach and its associated tools, Geophys. J. Int., 105, 271-284, 1991.

Pulliam J., and R.K. Snieder, Fast, efficient calculation of rays and travel times with ray perturbation theory, J. Acoust. Soc. Am., 99, 383-391, 1996.

Snieder, R.K., and M. Sambridge, The ambiguity in ray perturbation theory, J. Geophys. Res., 98, 22021-22034, 1993.

Villaseñor, A., M.H. Ritzwoller, A.L. Levshin, M.P. Barmin, E.R. Engdahl, W. Spakman and J. Trampert, Shear velocity structure of Central Eurasia from inversion of surface wave velocities, Phys. Earth Planet Int., submitted, 2000.

Widiyantoro, S., A. Gorbatov, B.L.N. Kennett, and Y. Fukao, Improving global shear wave traveltime tomography using three-dimensional ray tracing and iterative inversion, Geophys. J. Int., 141, 747-758, 2000.
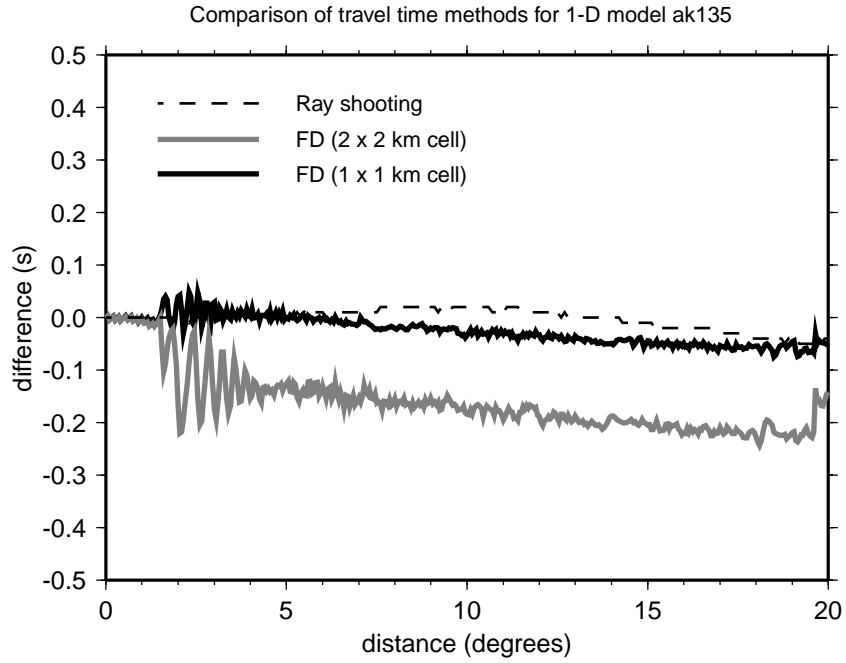
Figure 1. Differences between computed travel times using different methods and theoretical arrival times for the one dimensional model ak135. Thick black line for the finite difference method with 1 x 1 km cells, thick gray line for the same method with 2 x 2 km cells, and dashed line for the ray-shooting method.
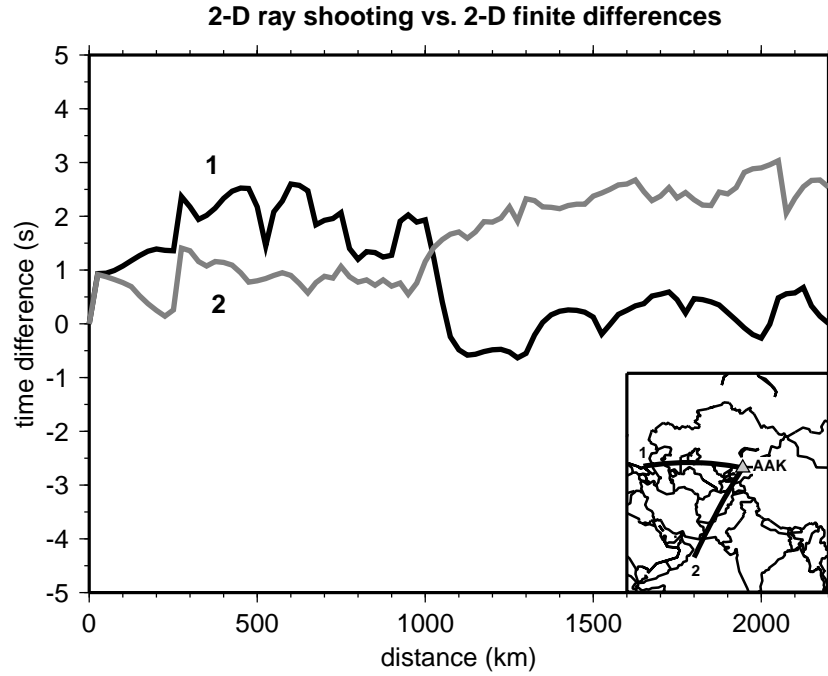
Figure 2. Differences between travel times computed using the 2-D ray shooting and the 2-D finite difference methods for two great circle cross sections through the vSV model of Villaseæor et al. (2000). The starting point of both great circle cross sections is IMS station AAK (Ala-Archa, Kyrgyzstan). The curves represent the ray-shooting travel time minus the finite difference travel time. Map inset shows the location of the two cross sections.
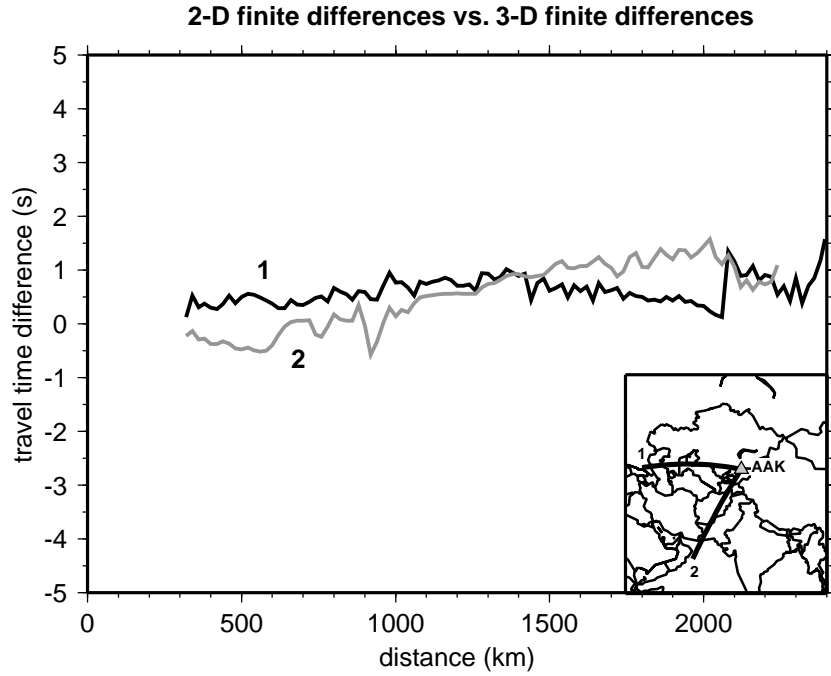
Figure 3. Differences between computed travel times along two great circle cross sections through the vSV model of Villaseæor et al. (2000) using the finite difference method in 2-D and 3-D. The starting point of both cross sections is IMS station AAK (Ala-Archa, Kyrgyzstan). Each curve represents the 2-D travel time minus the 3-D travel time. Map inset shows the location of the two cross sections.

Difference in P wave travel times

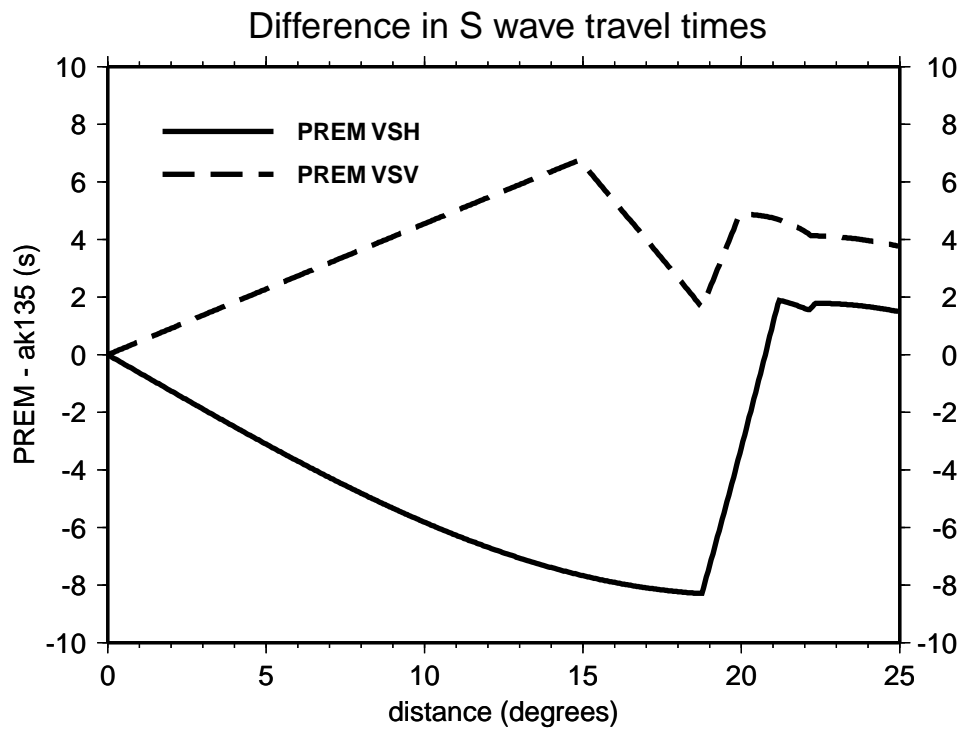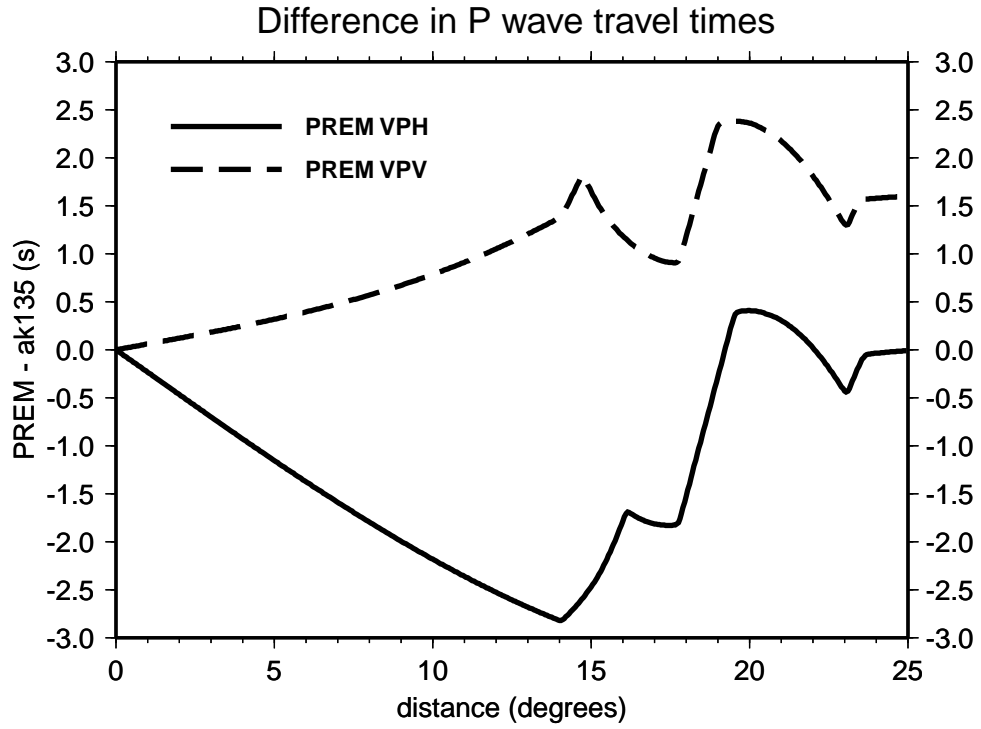

Difference in S wave travel times

Figure 4. Travel time differences between 1-D models PREM and ak135 for regional distances. Top panel shows differences in P-wave traveltimes, and bottom panel shows differences in S-wave travel times.
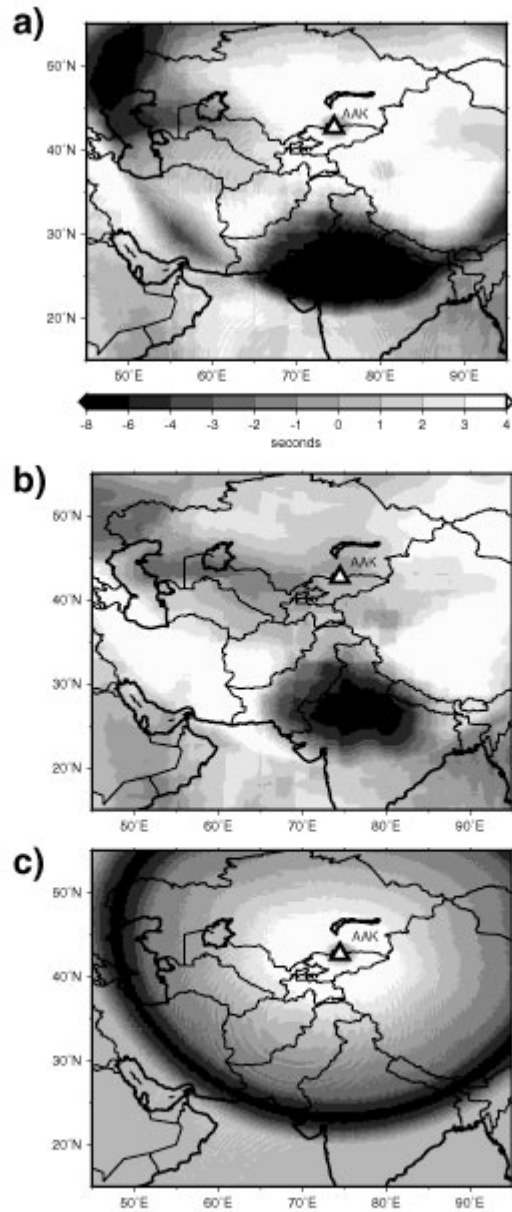
Figure 5. SSSCs for IMS station AAK (Ala-Archa, Kyrgyzstan) for the vSV model of Villaseñor et al. (2000). a) correction surface relative to ak135, b) relative to the model beneath the station, and c) difference between the two SSSCs.